

# MB-OFDM UWB over fiber system with direct detection

Jing He (何晶)\*, Xuejie Wen (温学杰), and Lin Chen (陈林)

Key Laboratory for Micro-/Nano-Optoelectronic Devices, Ministry of Education, College of Computer Science and Electronic Engineering, Hunan University, Changsha 410082, China

\*Corresponding author: hnu\_jhe@hotmail.com.

Received May 26, 2014; accepted July 16, 2014; posted online January 19, 2015

We experimentally demonstrate the multiband orthogonal frequency-division multiplexing ultra-wideband (MB-OFDM UWB) over fiber system with direct detection. Different sub-carrier modulation formats (quadrature phase shift keying (QPSK) and 16 quadrature amplitude modulation (QAM)) are investigated in the MB-OFDM UWB over fiber system. The experimental results show that a 3.84 Gb/s 16 QAM-encoded MB-OFDM UWB signal can be successfully transmitted over 70 km standard single-mode fiber without chromatic dispersion compensation.

OCIS codes: 060.2330, 060.4510.

doi: 10.3788/COL201513.S10604.

Multiband orthogonal frequency-division multiplexing ultra-wideband (MB-OFDM UWB) over fiber system has paid more and more attention in the future broadband wireless communication owing to its capability to decrease the frequency selective fading caused by multipath effect<sup>[1–3]</sup>. Meanwhile, it can increase the area of coverage and provide high-speed data transmission<sup>[4–8]</sup>. Yee *et al.*<sup>[5]</sup> found that directly modulated laser-based MB-OFDM UWB signals can transmit over up to 5 km of standard single-mode fiber (SSMF). Moreover, MB-OFDM UWB signals based on external modulation can transmit up to 40 km of SSMF<sup>[6]</sup>. However, highly received optical power is required. As it is known, MB-OFDM UWB signal can share the spectrum with the existing radio communications systems. Hraimel *et al.*<sup>[7]</sup> investigated the performance of MB-OFDM UWBoF transmission system, considering the effect of in-band narrowband jammers such as WiMAX, MIMO WLAN, WLAN, and marine radar. But it does not take into account the influence of first three bands of MB-OFDM UWB signal. Omomukuyo *et al.*<sup>[8]</sup> experimentally demonstrated the MB-OFDM UWB system applying digital pre-distortion scheme to improve transmission performance of the system. However, only first sub-band is studied.

In this letter, we experimentally investigate the performance of MB-OFDM UWB signal transmission over fiber system. The first three sub-bands of MB-OFDM UWB signal transmission performance are evaluated by measuring the receiver sensitivity, error vector magnitude (EVM), and constellation diagram. The experimental results show that 3.84 Gb/s 16 quadrature amplitude modulation (QAM)-encoded MB-OFDM UWB signals can be successfully transmitted over 70 km SSMF without chromatic dispersion compensation.

The American Federal Communications Commission was the first to open radio spectra of 3.1–10.6 GHz

with a spectrum width of 7.5 GHz for UWB use<sup>[9]</sup>. In the IEEE 802.15.3a standard, the spectrum width of MB-OFDM UWB signal is divided into 14 bands, and each band has a bandwidth of 528 MHz. The 14 channels are organized into five groups, as shown in Fig. 1. Each group has three channels from groups one to four and only two channels in group five. In fact, due to the constraint of current hardware, only the first three bands are investigated. Moreover, the center frequencies of the first three bands are  $f_1 = 3.432$  GHz,  $f_2 = 3.960$  GHz, and  $f_3 = 4.488$  GHz, respectively. To transmit three sub-bands of the MB-OFDM UWB signals simultaneously, the signal follows simple frequency-hopping sequences, such as  $f_1$ ,  $f_3$ , and  $f_2$ . Figure 2 shows the three bands with time–frequency code (TFC2) in the time domain<sup>[9]</sup>.

The architecture of the MB-OFDM UWB over fiber system is shown in Fig. 3. In the transmitter, the continuous light wave from the external cavity laser (ECL) is modulated by a Mach–Zehnder modulator (MZM). The pseudo-random binary sequences (PRBSs) are fed into an interleaver. Then, the output bits are mapped into quadrature phase shift keying (QPSK) or 16 QAM symbols. After inserting the pilots, the digital baseband OFDM symbol can be constructed by using inverse fast Fourier transform (IFFT). Therefore, the baseband OFDM symbol can be written as

$$S_{\text{BB-OFDM}}(t) = \sum_{k=-\frac{N_{\text{ST}}}{2}+1}^{\frac{N_{\text{ST}}}{2}} C_k \exp(j2\pi f_k t), \quad (1)$$

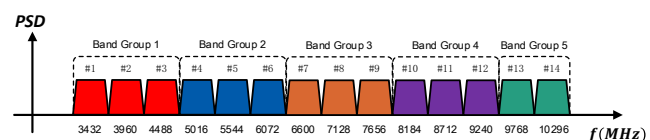


Fig. 1. Spectrum of MB-OFDM UWB signal band groups.

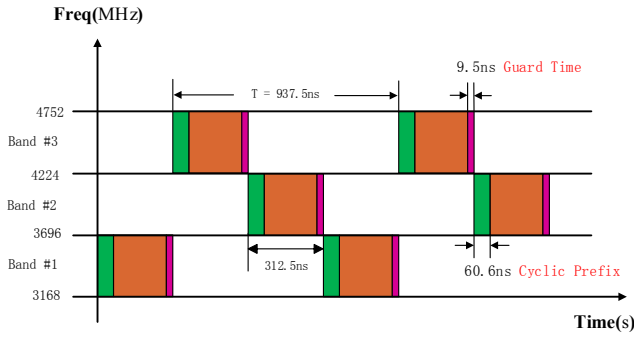


Fig. 2. Time–frequency representation of MB-OFDM UWB symbols with TFC2 = (1, 3, 2).

where  $N_{ST}$  is the total number of sub-carrier, and the frequency of the  $k$  sub-carrier is  $f_k$ . After adding the cyclic prefix (CP), digital-to-analog conversion (DAC), and intermediate frequency (IF) up-conversion with TFC, the IF MB-OFDM UWB signal is used as a radio frequency to the MZM. In addition, the IF MB-OFDM UWB signal can be expressed as

$$S_{\text{Elec-UWB}}(t) = \text{Re} \left\{ \sum_{n=1}^N \sum_{k=-\frac{N_{ST}}{2}+1}^{\frac{N_{ST}}{2}} \left[ C_k \exp(j2\pi f_k(t - nT_{\text{SYM}})) \right] \cdot \exp(j2\pi f_{\text{IF}}[q(n)]t) \right\}, \quad (2)$$

where  $f_{\text{IF}}[q(n)]$ ,  $N$ , and  $T_{\text{SYM}}$  are the carrier frequency functions of the MB-OFDM UWB signal, the number of OFDM symbols, and the symbol period, respectively.  $\text{Re}[\cdot]$  represents the real value of the electrical MB-OFDM UWB signal and  $q(n)$  is a function that maps the  $n$ th OFDM symbol to the appropriate frequency with TFC.

Consequently, the MB-OFDM UWB signal is applied to the MZM to modulate a light wave with an optical power  $P_{\text{in}}$  and a random phase  $\varphi_c(t)$  at an optical carrier frequency  $f_c$ . The relationship between MZM driving voltage and optical field at MZM output is given by

$$S_{\text{Opt-UWB}}(t) = \sqrt{2P_{\text{in}}} \cos(2\pi f_c t + \varphi_c(t)) \cdot \left[ \frac{\pi S_{\text{Ele-UWB}}(t) + V_{\text{bias}}}{2V_{\pi}} \right], \quad (3)$$

where  $V_{\text{bias}}$  denotes the direct current (DC) bias voltage, which is introduced to enable the MB-OFDM UWB demodulation using the direct detection and  $V_{\pi}$  is the voltage required to induce a  $\pi$  phase shift at the MZM.

At the receiver, the generated photocurrent  $I(t)$  of the photo-detector (PD) can be expressed as

$$\begin{aligned} I(t) &= \Re \left[ (S_{\text{Opt-UWB}}(t) + n(t)) * h(t) \right]^2 \\ &= \Re \left\{ \left[ S_{\text{Opt-UWB}}(t) * h(t) \right]^2 + \left[ n(t) * h(t) \right]^2 + 2 \text{Re} \left[ (S_{\text{Opt-UWB}}(t) * h(t)) * (n(t) * h(t)) \right] \right\}, \end{aligned} \quad (4)$$

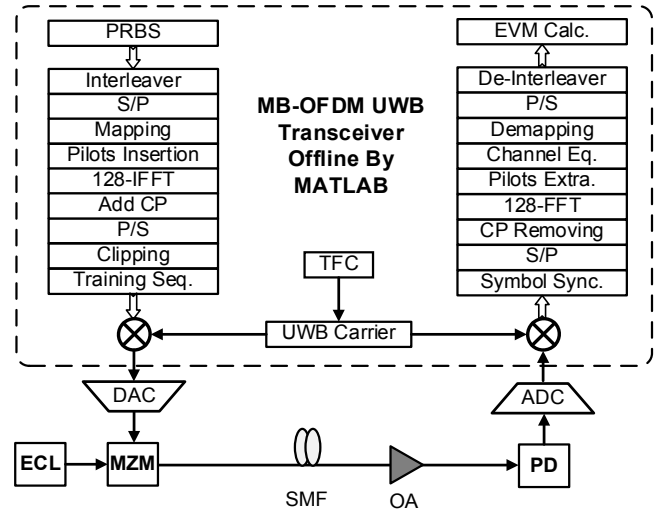


Fig. 3. Structure of MB-OFDM UWB over fiber system.

where  $\Re$  is the responsivity of the PD,  $n(t)$  is the noise of optical amplifier, and  $h(t)$  is the impulse response of the transmitted channel. The electrical signal is downconverted to the baseband signal with the corresponding TFC. After the analog-to-digital conversion (ADC) and symbol synchronization, the baseband digital signal processing includes the FFT, pilot-aided channel estimation, equalization, and demapping. Before the demodulation, the EVMs on the data-carrying sub-carriers are calculated to evaluate the system performance.

The experimental setup of the MB-OFDM UWB over fiber system is shown in Fig. 4. In the central station, continuous wave (CW) light is generated from a commercial ECL source at the wavelength of 1565.38 nm and an output power of 7 dBm. Then the CW light is injected into a single-electrode MZM, which is driven by the electrical MB-OFDM UWB signal. The MB-OFDM UWB signal is generated offline by MATLAB and then loaded into an arbitrary waveform generator (AWG) operating at 10.56 Gsamples/s. In addition, the total number of sub-carriers is 128, where the sub-carriers used for data, pilots, nulls, and guard intervals are 100, 12, 6, and 10, respectively. QPSK and 16 QAM modulations are alternatively employed for sub-carriers modulation. Thus, the modulating MB-OFDM UWB signal spans from 3.168 to 4.752 GHz. It comprises three 528 MHz-wide sub-bands. And the bit rate of each sub-band is 1.28 Gb/s, resulting in an aggregate bit rate of 3.84 Gb/s when 16 QAM is used to sub-carrier modulation<sup>[10]</sup>. Here, the polarization controller is used to ensure maximum amplitude of the optical carrier. In addition, the MZM ( $V_{\pi} = 4$  V) has an insertion loss

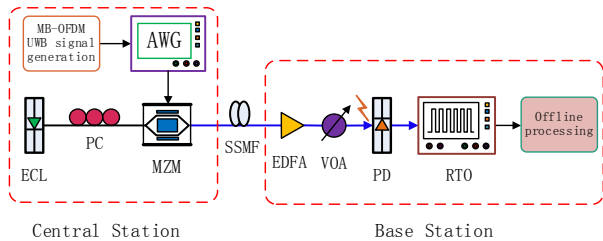


Fig. 4. Experimental setup of the MB-OFDM UWB over fiber system.

of 6 dB, and  $V_{\pi}$  is the voltage to induce a  $\pi$  phase shift at the MZM. The DC bias voltage of the MZM biased at quadrature point is 1.6 V. After modulating by MZM, the output optical MB-OFDM UWB signal is then transmitted over 70 km SSMF with fiber loss of 0.2 dB/km and chromatic dispersion of 17 ps/(nm.km).

At the base station, the optical signal is amplified to 6 dBm by an erbium-doped fiber amplifier with a noise figure of 5 dB to compensate the fiber and connector losses. The variable optical attenuator (VOA) is varied to calculate the EVM of the signal as a function of the received optical power. Then, the optical to electrical conversion is achieved by a commercial PD with a 3 dB bandwidth of 10 GHz. The converted electrical MB-OFDM UWB signal is sampled by a Tektronix, 8 GHz, real-time oscilloscope operated at 20 Gsamples/s. Consequently, the received MB-OFDM UWB samples are offline processing including equalization, demodulation, demapping 16 QAM (QPSK) signal, and EVM calculation by MATLAB.

The waveform of measured MB-OFDM UWB signal is shown in Fig. 5 at -13 dBm of received optical power. The EVM of MB-OFDM UWB signal with different modulation formats (QPSK and 16 QAM), as a function of received optical power is shown in Fig. 6. It can be seen that the EVM performance is degraded as the received optical power decreases. Compared with 16 QAM modulation format, the

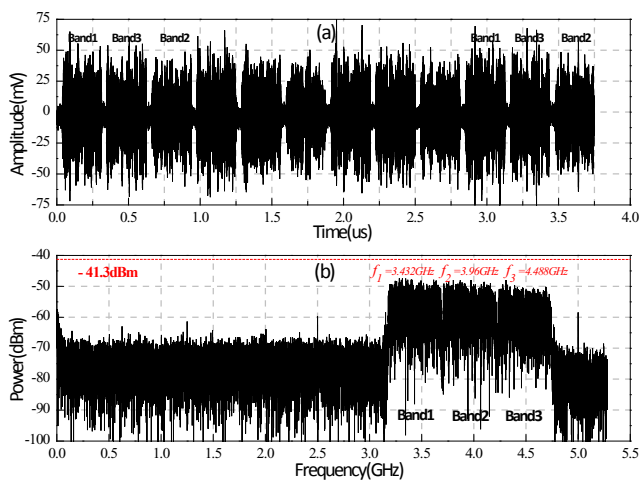


Fig. 5. Waveform of the received MB-OFDM UWB signal in (a) time and (b) frequency domain.

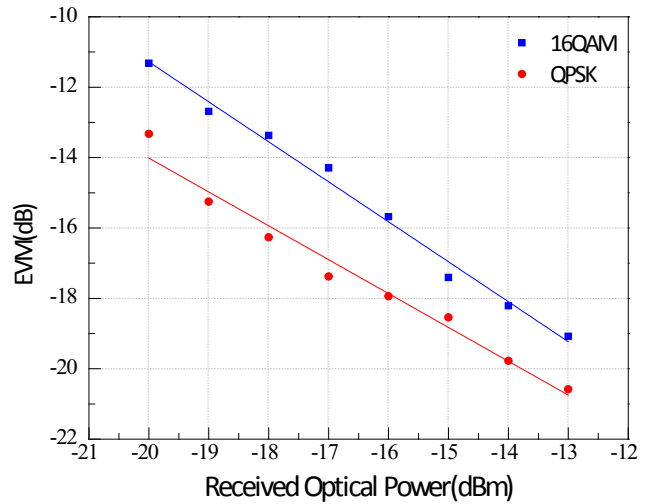


Fig. 6. EVM of MB-OFDM UWB signal for fixed SSMF length of 70 km.

received sensitivity of QPSK modulation is improved about 2 dB at the EVM of -17 dB. Considering that the received optical powers are -13 and -20 dBm after 70 km SSMF transmission, the constellation diagrams of the two modulation formats are shown in Fig. 7. The constellation diagrams of QPSK and 16 QAM have serious deviation due to the chromatic dispersion of the fiber and optical amplifier noise. It is clearly seen that the performance of QPSK format is better than that of the 16 QAM at all of the received optical power. However, the bit rate of MB-OFDM UWB signal using QPSK format is only half of 16 QAM format.

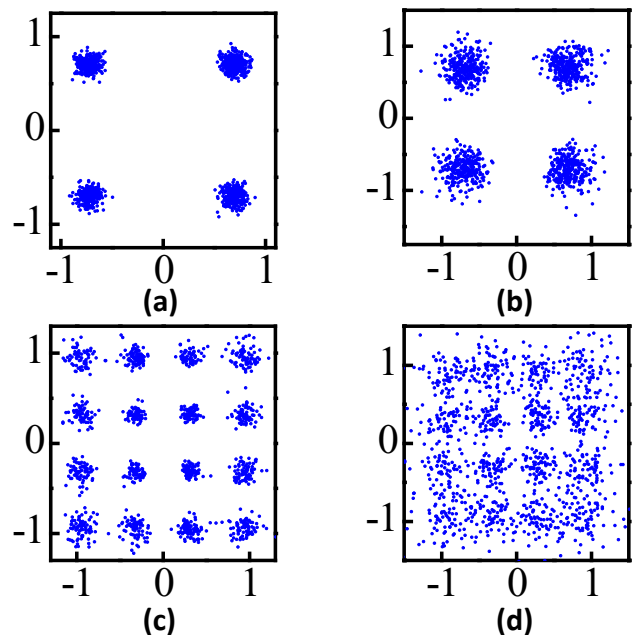


Fig. 7. Constellation diagrams of fiber transmission for different received optical powers after 70 km SSMF: (a) QPSK, -13 dBm, (b) QPSK, -20 dBm, (c) 16 QAM, -13 dBm, and (d) 16 QAM, -20 dBm.

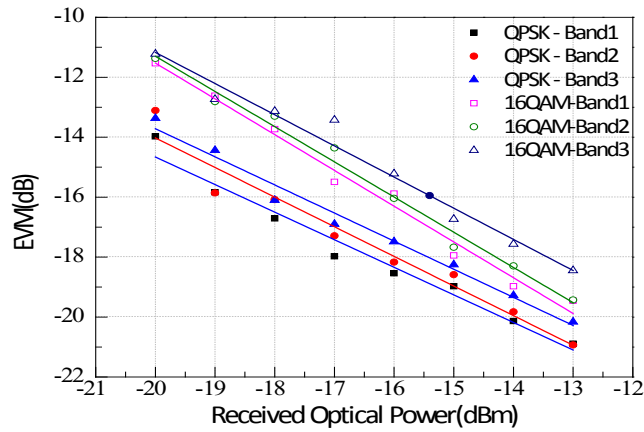


Fig. 8. EVM of first three MB-OFDM UWB sub-bands for a fixed SSMF length of 70 km.

Figure 8 shows the EVM of the received first three MB-OFDM UWB sub-bands. The higher order sub-band is impressionable by chromatic dispersion of the fiber at the received power of  $-13$  dBm. Comparing band 1 with band 3, the gain of both the QPSK and 16 QAM format is found to be 2 dB. With the decrease in the received power, the EVM is limited by electrical noise. The constellation diagrams of the two modulations are serious distortion at the received power of  $-20$  dBm. Therefore, the trend of EVM curves maybe to converge.

In conclusion, we experimentally investigate the performance of MB-OFDM UWB over fiber system. A 3.84 Gb/s 16 QAM-encoded MB-OFDM UWB signal can be successfully transmitted over 70 km SSMF without chromatic dispersion compensation. Compared with

16 QAM format, the received sensitivity of QPSK format is improved to about 2 dB at the EVM of  $-17$  dB. However, the higher order sub-band is impressionable by chromatic dispersion of the fiber.

This work was supported by the National Natural Science Foundation of China (Nos. 61307087 and 61377079), the Hunan Provincial Natural Science Foundation of China (No. 12JJ3070), and the Fundamental Research Funds for the Central Universities and Young Teachers Program of Hunan University.

## References

1. G. R. Aiello and G. D. Rogerson, *Microw. Mag.* **4**, 2 (2003).
2. Federal Communications Commission, "Revision of part 15 of the Commission's rules regarding ultra-wideband transmission systems," FCC 02-48 (2002).
3. Eema International Standard ECMA-368, High Rate Ultra Wide-band PHY and MAC Standard(2008).
4. J. Yu, M. F. Huang, D. Qian, L. Chen, and G. K. Chang, *Photon. Technol. Lett.* **20**, 18 (2008).
5. M. L. Yee, V. H. Pham, Y. X. Guo, L. C. Ong, and B. Luo, in *Proceedings of IEEE International Conference on Ultra-Wideband* 674 (2007).
6. M. N. Sakib, B. Hraimel, X. Zhang, M. Mohamed, W. Jiang, K. Wu, and D. Shen, *J. Lightw. Technol.* **27**, 18 (2009).
7. B. Hraimel, X. Zhang, and Y. Shen, in *Proceedings of Optical Fiber Communication Conference 2010 OTuF4* (2010).
8. O. Omomukuyo, M. P. Thakur, and J. E. Mitchell, in *Proceedings of Asia Communications and Photonics Conference ATHC-4* (2012).
9. IEEE P802.15-03/268r2, Multi-Band OFDM physical layer proposal for IEEE 802.15 Task Group 3a (2004).
10. O. Omomukuyo, M. P. Thakur, and J. E. Mitchell, *Photon. Technol. Lett.* **25**, 3 (2013).